Available online at www.sciencedirect.com

ScienceDirect

Ceramics International 40 (2014) 1741–1746

CERAMICS INTERNATIONAL

www.elsevier.com/locate/ceramint

Comparative study of an experimental Portland cement and ProRoot MTA by electrochemical impedance spectroscopy

Kyung-Pil Seong[a], Sang-Yun Jeon[a], Bhupendra Singh[a,b], Jin-Ha Hwang[c], Sun-Ju Song[a,b,*]

[a]School of Materials Science and Engineering, Chonnam National University, 300 Yongbong-dong, Buk-gu, Gwang-Ju 500-757, Republic of Korea
[b]Research Institute for Catalysis, Chonnam National University, Gwang-Ju 500-757, Republic of Korea
[c]Department of Materials Science and Engineering, Hongik University, Seoul 121-791, Republic of Korea

Received 17 June 2013; received in revised form 15 July 2013; accepted 15 July 2013
Available online 23 July 2013

Abstract

An experimental Portland cement (EPC) was manufactured with pure raw materials under controlled laboratory conditions. The physical properties and biocompatibility of EPC was compared with that of ProRoot MTA. The microstructure and chemical composition of EPC was analyzed by scanning electron microscopy (SEM) and X-ray diffraction (XRD) respectively. The cytotoxicity of the extracts of EPC and ProRoot MTA on MG-63 cells was evaluated by using a 2,3-bis(2-methoxy-4-nitro-5-sulfophenyl)-5-[(phenylamino)carbonyl]-2H-tetrazolium hydroxide (XTT) assay. The setting process was monitored by electrochemical impedance spectroscopy (EIS) and the electrical responses obtained with respect to time were analyzed using equivalent circuit models to separate bulk and electrode response. The EPC paste showed higher electrical conductivity than ProRoot MTA and it set slowly, which could be due to the presence of excess CaO in EPC composition.

Keywords: Dental cement; Electrochemical impedance spectroscopy; Experimental Portland cement; ProRoot MTA

1. Introduction

A number of studies have shown that mineral trioxide aggregate (MTA) shows good physical, chemical, mechanical and biological properties for its application in dental surgery [1,2]. MTA has been widely used in root canal sealing [3], iatrogenic root perforations [4,5], root-end fillings [6,7] and pulpotomy [8,9]. However, its higher cost, handling difficulty and longer setting time have been major impediments to its widespread use [10–12].

Due to the composition similarity with MTA [12], Portland cement (PC) has been analyzed and compared with MTA and it has been considered as alternative to MTA [7,12]. However, one important point in the development of PC-based low-cost dental material is the concerns against the presence of the toxic heavy metal in PC which prevents its wide acceptance as its dental use [13,14]. Currently, the goal of several studies is to formulate a material based on MTA or Portland cement to be used in dental surgery at a lower cost and with shorter processing time and minimal cytotoxic implications [15]. Several compositional manipulations have been made in already existing commercial dental cements, and consequently several biological, chemical, and physical tests have been conducted to assess their properties [16–20]. But, not many efforts have been made to develop new endodontic cement from pure raw materials, which incorporates the advantages of both MTA and PC at a lower cost. In our previous work, however, we prepared an experimental PC and its physical properties and biocompatibility were compared with those of MTA and ordinary PC [16].

XRD has been used to identify the crystalline structures of cement-based materials. XRD analyses of PC have shown that tricalcium silicate, tricalcium aluminate and calcium silicate are the major constituents of PC [12,21]. Each constituent has characteristic diffraction patterns and there may be multiple overlapping peaks in each sample, owing to the fact that cement consists of several chemical compounds. Therefore, it is not

*Corresponding author at: School of Materials Science and Engineering, Chonnam National University, 300 Yongbong-dong, Buk-gu, Gwang-Ju 500-757, Republic of Korea. Tel.: +82 62 530 1706; fax: +82 62 530 1699.
E-mail address: song@chonnam.ac.kr (K.-P. Seong).

0272-8842/$ - see front matter © 2013 Elsevier Ltd and Techna Group S.r.l. All rights reserved.
http://dx.doi.org/10.1016/j.ceramint.2013.07.073

possible to quantify each constituents using XRD, qualitative identification of major components is possible by XRD.

By the virtue of its interconnected pore network filled with mobile ion containing water, cement paste is electrically conductive. During the setting process the pore structure is continuously altered and affects the electrical conductivity of the cement [22]. Frequency-dependent impedance spectroscopy has been used for in situ monitoring of hydration process in cement-based materials [22–24]. Because of non-destructive characteristics of EIS, data acquisition does not interrupt with the setting process and therefore long term monitoring of the electrical properties is possible during the setting process [25].

The objective of the present study is to perform further studies on EPC in order to test its applicability as a potential substitute for commercially available expensive dental cements. In the present study, we use frequency dependent EIS to analyze the setting process of EPC and MTA. Furthermore, the chemical composition and microstructure of EPC was analyzed by XRD and SEM, respectively, and the degree of cytotoxicity was evaluated by XTT assay. Various results for EPC were compared with those for ProRoot MTA.

2. Experimental

2.1. Synthesis of EPC

The EPC was synthesized in laboratory under controlled and clean conditions with pure raw materials to ensure that the final products were free of undesirable ingredients. The purity and mix ratio of the various raw materials used in the EPC synthesis are listed in Table 1. Fig. 1 shows the flow chart of various steps involved in the manufacture of EPC. Briefly, all the raw materials were mixed in the appropriated ratio as mentioned in Table 1 and ground by ball-milling in isopropyl alcohol (IPA) with zirconia balls for 1 day. The obtained mixture was dried in hot air oven for 1 day at 80 °C and again moistened with 15 wt% of IPA to get semi-dried slurry. Spherical pellets of 1.5 cm diameter were formed from the semi-dried slurry and the spheres were dried in hot air oven at 80 °C for 1 day. The dried spheres were stepwise sintered at different temperatures (at 600 °C for 30 min→at 900 °C for 15 min→at 1300 °C for 15 min→at 1450 °C for 1 h) and then quenched to room temperature in liquid nitrogen. The heating rate during sintering was fixed at 3 °C/min in air. The time schedule used for stepwise sintering was provided by the Eugene Corporation, Korea [26]. The clinker obtained by quenching was fully ground and sieved stepwise by 100, 75 and 38 μm mesh-size test sieves to get EPC powder. The MTA used for comparison was ProRoot MTA (Dentsply Tulsa Dental Specialities, Tulsa, OK, USA).

2.2. Structural characterization

The phase composition of EPC powder was analyzed by high resolution X-ray diffractometer (D/Max Ultima III, Rigaku, Japan) equipped with a Cu-K_α radiation source (1.5406 Å) at a scan rate of 1°/min between scanning angles (2θ) of 10–90° and the phase identification was accomplished by matching the experimental XRD data with the Inorganic Crystal Structure Database (ICSD) of Korea Institute of Science and Technology Information. The microstructures of EPC and ProRoot MTA were analyzed using a field-emission scanning electron microscope (FE-SEM, S-4700, Hitachi).

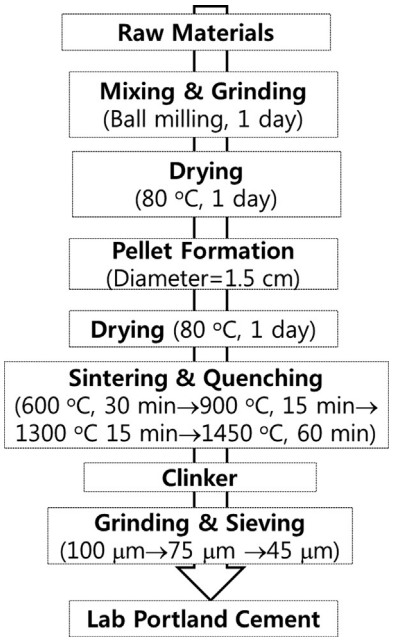

Fig. 1. Flow chart of various steps involved in synthesis of EPC.

Table 1
Details of raw materials used in synthesis of EPC.

Raw materials	Purity (%)	Manufacturers	Mix ratio (%)
CaO	98	Hayashi Pure Chemical, Japan	64.84
SiO_2	99.9	Semiconductor Materials Corp. Japan	21.59
Al_2O_3	98	Katayama Chemical, Japan	4.8
Fe_2O_3	99	Yakuri Pure Chemical, Japan	3.56
MgO	98	Shinyo Pure Chemical, Japan	3.76
K_2CO_3	99.5	Hayashi Pure Chemical, Japan	1.38
[a]Na_2O	80	Sigma-Aldrich, USA	0.08

[a]The purity of Na_2O was 80% and the other 20% was present as Na_2O_2.

2.3. Cytotoxicity test

The cytotoxicity of the EPC and ProRoot MTA was performed by XTT assay. The details about cell culture, material preparation and XTT assay are similar to as reported elsewhere [16].

2.4. Electrochemical measurements

The electrochemical analysis of the setting process of EPC was performed by the EIS. The EPC specimens for the EIS were prepared in specimen fixture (16 mm × 16 mm × 10 mm) made of acrylic panel, as shown in Fig. 2. The thickness of acrylic panel was 3 mm. 1.0 g power of EPC was hand-mixed with 0.3 g water while tapping in the container for 30 s and poured into the specimen fixture and covered. Two planar stainless steel electrodes were inserted (contact area 0.58 cm^2) into the pastes contained in a rectangular box. For the protecting of evaporation of water, surrounding of fixture was glued by the silicon glue. The two electrodes were connected to a frequency-response analyzer (SI-1260, Solatron, England). Total handling time before the impedance measurement was 5 min. The ProRoot MTA specimens for the EIS were prepared in similar manner as described above for EPC. The impedance spectra were collected as a function of frequency at 10 points per decade in a logarithmic manner between 10 MHz and 0.1 Hz using Z60 software.

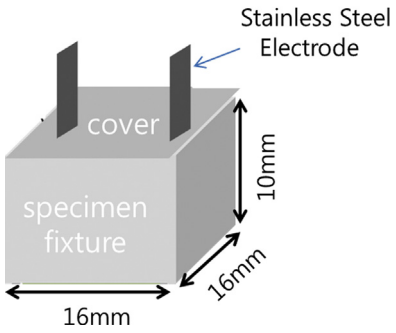

Fig. 2. Schematic of module used for EIS measurements.

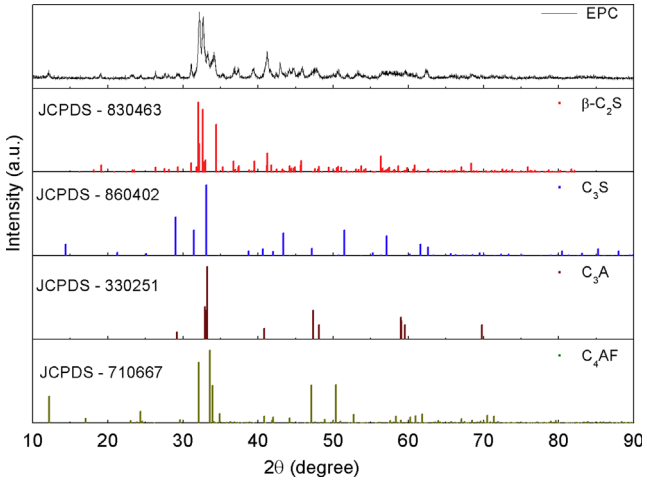

Fig. 3. XRD patterns of EPC, β-C_2S, C_3S, C_3A and C_4AF.

3. Results and discussion

Fig. 3 shows the XRD pattern of EPC powder along with the reference data for β-$2CaO \cdot SiO_2$ (β-C_2S), $3CaO \cdot SiO_2$ (C_3S), $3CaO \cdot Al_2O_3$ (C_3A) and $4CaO \cdot Al_2O_3 \cdot Fe_2O_3$ (C_4AF). Slightly broad multiple peaks were observed at 32–34° which can be assigned to β-C_2S. Peaks at 29.38°, 31.2°, 33.4° and 51.9° can be assigned to C_3S. Peaks at 33.25°, 47.59° and 59.53° can be indicative of C_3A whereas peaks at 12.09°, 24.42°, 50.52° and 51.99° can be assigned to C_4AF. The XRD results show that all 4 major constituents of cement are present in the EPC.

Fig. 4 shows SEM images of EPC (a) and ProRoot MTA (b). As can be seen, the microstructure of EPC was similar to that of ProRoot MTA and both are composed of relatively inhomogeneous aggregates. The figures in inset show that aggregates are composed of smaller particles.

Fig. 5 shows the cell viability of MG-63 cells with an extract from the test materials. As can be seen, EPC and ProRoot MTA showed similar cytotoxicity to the MG-63 cells and none of them exhibited significant cytotoxicity for up to 7 days. The XTT assay showed that EPC and ProRoot MTA were biocompatible when exposed to human osteosarcoma cells. The cells cultured for 24 h on EPC were viable and proliferated in direct contact with the cement surfaces.

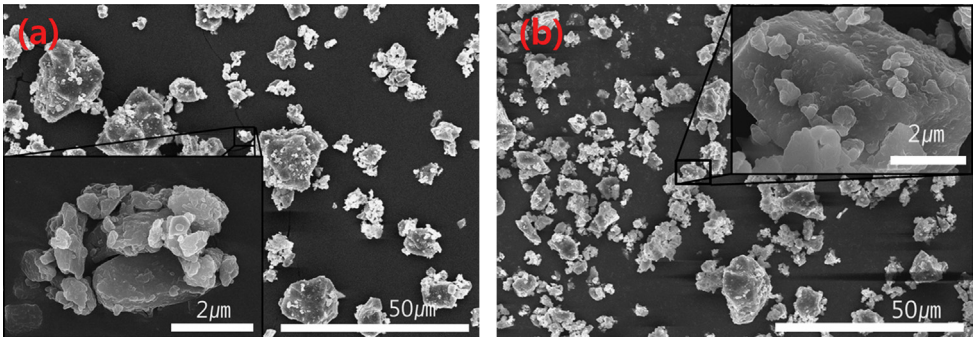

Fig. 4. SEM image of (a) ProRoot MTA and (b) EPC.

The impedance spectra of various samples were collected as a function of setting time, as shown in Fig. 6. Fig. 6(a) and (b) shows the impedance spectra of ProRoot MTA and, as can be seen the high frequency impedance increases with the time. The high frequency impedance is attributed to the bulk response [25,27], indicating the overall resistance of the sample increases with setting time. The setting process of cement based materials produces a continuously evolving solid network of high resistivity materials, such as calcium silicate hydrate, which is filled with the ion-conducting high-pH liquid phase obtained by the dissolution of ionic species in water. This overall combination of the structure of solid network (i.e. pore structure) and composition of ion-conducting liquid phase (i.e. pore solution) determines the electrical conductivity of the cement based materials during the setting process. During the setting process, the continuously increasing solid phase infringes into the liquid phase by the formation of silicate and hydrate products, thereby decreasing the amount of porous ion-conducting path. Therefore, in the impedance response of ProRoot MTA, the size of high frequency semi-circle keeps increasing as the setting-time laps, as can be seen in Fig. 6(a) and (b). The impedance response of initial setting process of EPC is given in Fig. 6(c) and the high frequency arcs show decreasing trend in their size as time laps for 1 day and it is only after 1 day the size of high frequency impedance arcs increases with setting-time, as shown in Fig. 6(c) and (d). As can be seen, the impedance response of the initial setting process of EPC is different from that of the ProRoot MTA and the possible reason for this difference will be discussed subsequently.

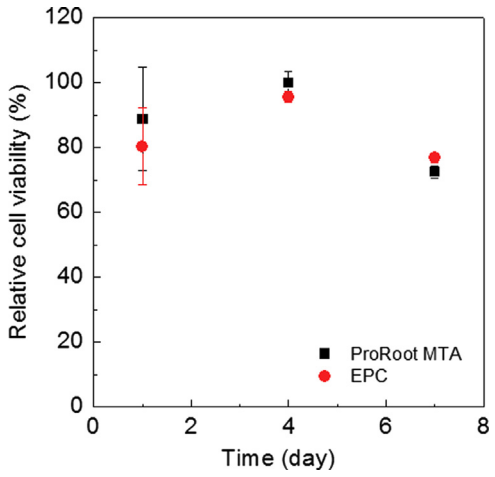

Fig. 5. Cell viability of MG-63 cells exposed to extracts from test materials as measured by XTT assay.

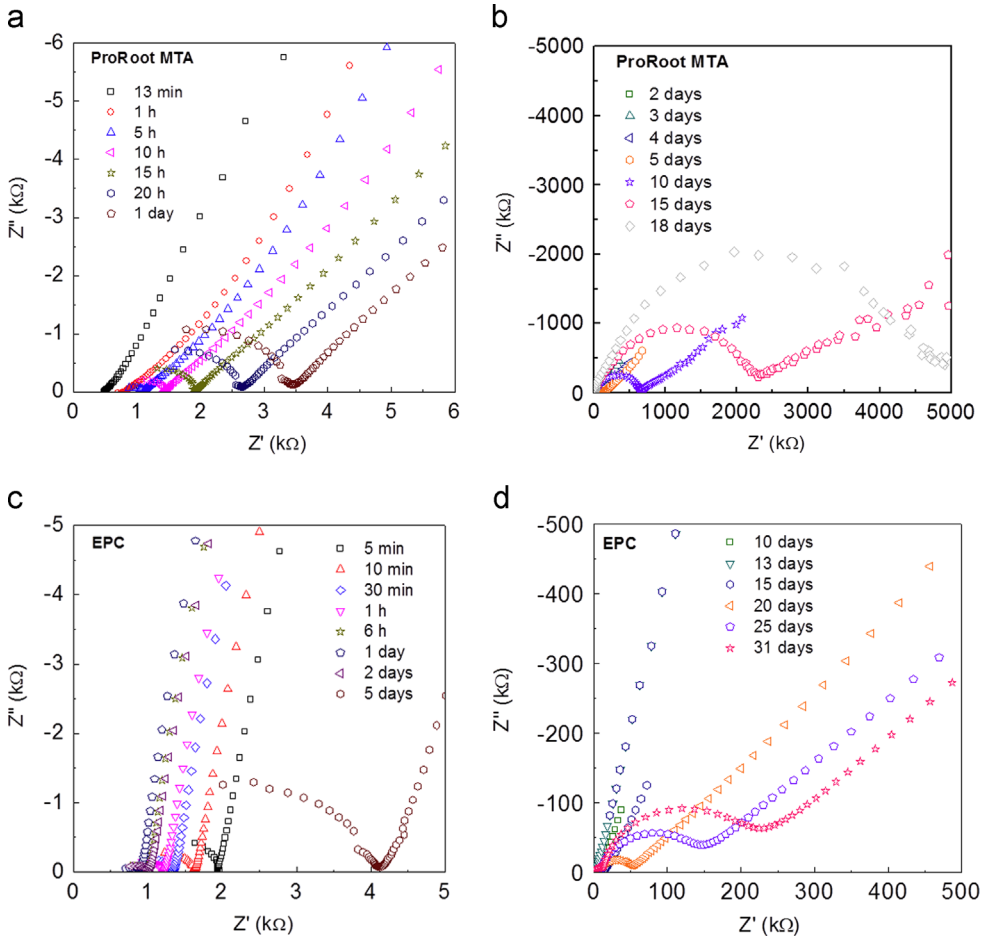

Fig. 6. Time dependent complex plane impedance response of ProRoot MTA (a, b) and EPC (c, d) during setting process.

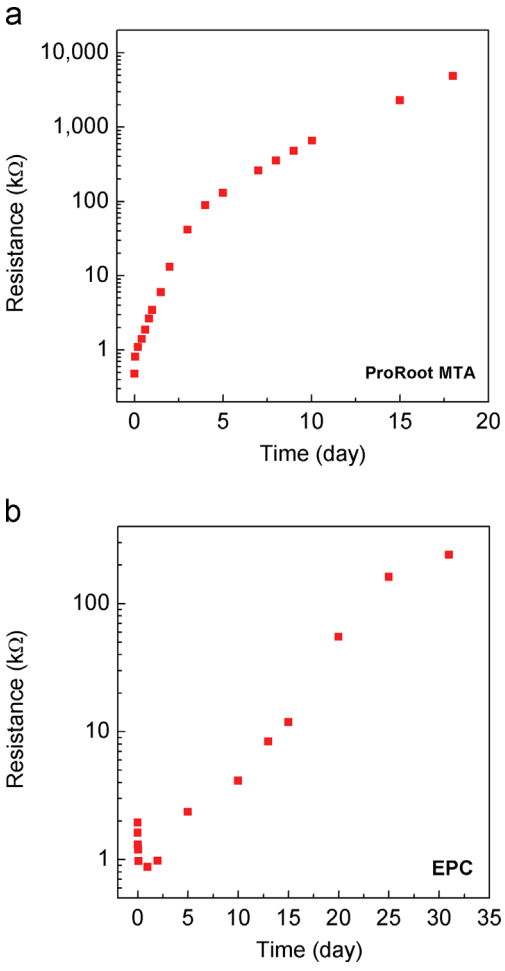

Fig. 7. Variation of resistance vs. time of (a) ProRoot MTA and (b) EPC during setting process.

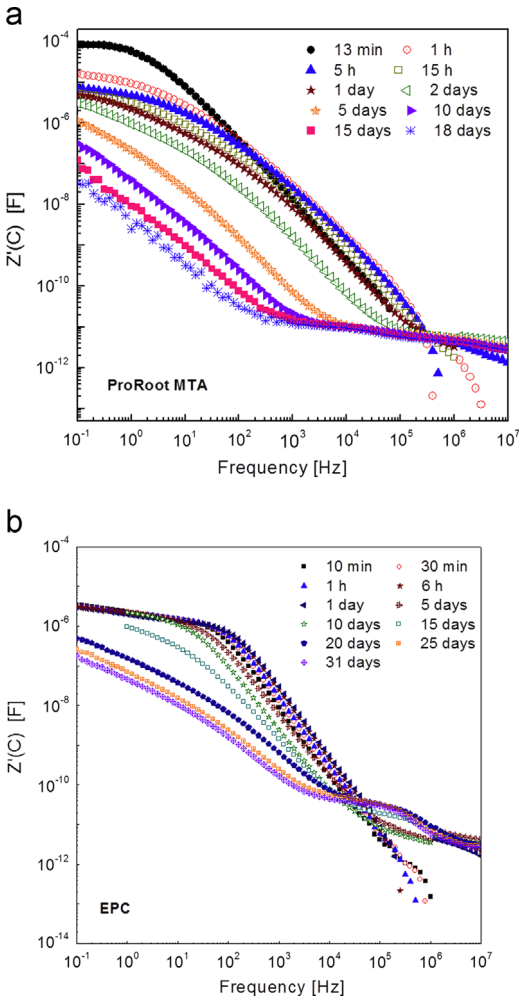

Fig. 8. Capacitance Bode plots as a function of frequency for (a) ProRoot MTA and (b) EPC.

The change in resistance of the samples with time during the setting process was calculated and is shown in Fig. 7. As can be seen in Fig. 7(a), the resistance of ProRoot MTA continuously increases with the time and this increase is very rapid during the initial 2 days from the onset of setting process. On the other hand, the resistance of the EPC in Fig. 7(b) initially decreases with the onset of the setting process before increasing with time and the increase in resistance with time is relatively slow in comparison to ProRoot MTA.

As stated earlier, the electrical conduction in cement based materials is dependent on the interconnectivity of the porous regions filled with ion-rich solution phase. The results in Fig. 7 indicate that upon hydration of ProRoot MTA the highly resistive solid fraction increases rapidly and with the onset of setting process the continuously evolving solid phases intrude into the pores and decreasing the interconnectivity of the ion-rich solution phase by forming a barrier of calcium–silicate–hydrate (C–S–H) gel phase, thereby decreasing the conductivity of the material. The difference in trend shown by EPC could be due to the presence of a small amount of unreacted or intrinsically formed CaO which increases the ionic conductivity of liquid phase and probably have deleterious effect on the setting process, thereby causing slow evolution of highly resistive phases and consequently slow decrease in interconnectivity of ion-rich solution phase. It is worth mentioning that although it is hard to identify any unreacted CaO phase in the XRD spectrum of EPC, because of its composite nature, its presence cannot be ruled out.

Fig. 8 shows the frequency-dependent capacitance Bode plots for hydration process of (a) ProRoot MTA and (b) EPC. In high frequency region, which corresponds to the bulk response, the capacitance was in picofarad range and initially it increases and then decreases with time upon hydration. As mentioned earlier, the hydration process leads to the formation of C–S–H gel phases. At the early times, when these barrier C–S–H phases are formed in the pores of the continuously developing network, the bulk capacitance increases due to the constriction of pore network and the voltage drop across C–S–H barriers. As the setting process continues, these barriers thicken and cause decrease in the bulk capacitance. With the passage of long time, the hydration process slows down and the bulk capacitance shows a plateau [28]. On the other hand, in Fig. 8 (a), the capacitance in low frequency region, which is the characteristic of the charge transfer between the electronic conductor and ion-rich solution phase, decreases with time due to the infringement of C–H–S gel phase into the ion-rich solution phase

[25]. The variation of bulk capacitance of EPC in Fig. 8(b) shows similar trend, except the appearance of stare-shaped plateau region which is indicative of thinner C–S–H barriers due to the slower setting process in EPC [28]. Similarly, the decrease in capacitance in low frequency region with time is slower in EPC than that in ProRoot MTA. Also, EPC shows nearly identical low frequency capacitance responses for ~5 days, which is indicative of good charge transfer between the electronic conductor and solution phase due to the high conductivity of ion-rich solution phase as well as slower rate of development of C–S–H barriers.

4. Conclusions

An experimental Portland cement was manufactured with pure raw materials under controlled laboratory conditions. The physical properties and biocompatibility of EPC was compared with that of ProRoot MTA. The microstructure and chemical composition of EPC was similar to that of ProRoot MTA. The biocompatibility of EPC was comparable to ProRoot MTA and the monitoring of hydration process by EIS, however, showed that EPC paste has high electrical conductivity and its rate of setting was slow, probably due to the presence of unreacted or intrinsically formed CaO. Further research is needed to optimize the composition of EPC in order to accelerate its setting process, so that it can be viable for dental applications.

Acknowledgment

This research was supported by the Basic Research Laboratories (BRL) Program (2011-0001567) of the National Research Foundation of Korea (NRF) and funded by the Korean Ministry of Education, Science and Technology (MEST).

References

[1] H.W. Roberts, J.M. Toth, D.W. Berzins, D.G. Charlton, Mineral trioxide aggregate material use in endodontic treatment—a review of the literature, Dental Materials 24 (2008) 149–164.
[2] J. Camilleri, T.R. Pitt Ford, Mineral trioxide aggregate—a review of the constituents and biological properties of the material, International Endodontic Journal 39 (2006) 747–754.
[3] S.J. Lee, M. Monsef, M. Torabinejad, The sealing ability of a mineral trioxide aggregate for repair of lateral root perforations, Journal of Endodontics 19 (1993) 541–544.
[4] G.C. Unal, M. Maden, T. Isidan, Repair of furcal iatrogenic perforation with mineral trioxide aggregate: two years follow-up of two cases, European Journal of Dentistry 4 (2010) 475–481.
[5] E.J. da Silva, C.V. Andrade, L.Y. Tay, D.R. Herrera, Furcal-perforation repair with mineral trioxide aggregate: two years follow-up, Indian Journal of Dental Research 23 (2012) 542–545.
[6] M. Torabinejad, T.F. Watson, T.R. Pitt Ford, Sealing ability of a mineral trioxide aggregate when used as a root end filling material, Journal of Endodontics 19 (1993) 591–595.
[7] S. Shahi, H.R. Yavari, S. Rahimi, M. Eskandarinezhad, S. Shakuouei, M. Unchi, Comparison of the sealing ability of mineral trioxide aggregate and Portland cement used as root-end filling materials, Journal of Oral Science 53 (2011) 517–522.
[8] M.A. Simancas-Pallares, A.J. Díaz-Caballero, L.M. Luna-Ricardo, Mineral trioxide aggregate in primary teeth pulpotomy. A systematic literature review, Medicina Oral, Patología Oral y Cirugía Bucal 15 (2010) e942–e946.
[9] A.P. Erdem, Y. Guven, B. Balli, B. Ilhan, E. Sepet, I. Ulukapi, O. Aktoren, Success rates of mineral trioxide aggregate, ferric sulfate, and formocresol pulpotomies: a 24-month study, Pediatric Dentistry 33 (2011) 165–170.
[10] M. Torabinejad, C.U. Hong, F. McDonald, T.R. Pitt Ford, Physical and chemical properties of a new root-end filling material, Journal of Endodontics 21 (1995) 349–353.
[11] B.R. Johnson, Considerations in the selection of a root-end filling material, Oral Surgery, Oral Medicine, Oral Pathology, Oral Radiology and Endodontology 87 (1999) 398–404.
[12] I. Islam, H.K. Chung, A.U. Yap, Comparison of the physical and mechanical properties of MTA and Portland cement, Journal of Endodontics 32 (2006) 193–197.
[13] G. De-Deus, M.C.B. de Souza, R.A.S. Fidel, S.R. Fidel, R.C. de Campos, A.S. Luna, Negligible expression of arsenic in some commercially available brands of Portland cement and mineral trioxide aggregate, Journal of Endodontics 35 (2009) 887–890.
[14] M.A. Duarte, A.C. De Oliveira Demarchi, J.C. Yamashita, M.C. Kuga, S. de Campos Fraga, Arsenic release provided by MTA and Portland cement, Oral Surgery, Oral Medicine, Oral Pathology, Oral Radiology and Endodontology 99 (2005) 648–650.
[15] N.V. Viola, M.T. Filho, P.S. Cerri, MTA versus Portland cement; review of literature, Revista Sul-Brasileira de Odontologia 8 (2011) 446–452.
[16] Y.C. Hwang, D.H. Kim, I.N. Hwang, S.J. Song, Y.J. Park, J.T. Koh, H.H. Son, W.M. Oh, Chemical constitution, physical properties, and biocompatibility of experimentally manufactured Portland cement, Journal of Endodontics 37 (2011) 58–62.
[17] S. Asgary, S. Shahabi, T. Jafarzadeh, S. Amini, S. Kheirieh, The properties of a new endodontic material, Journal of Endodontics 34 (2008) 990–993.
[18] M.G. Gandolfi, F. Perut, G. Ciapetti, R. Mongiorgi, C. Prati, New Portland cement-based materials for endodontics mixed with articaine solution: a study of cellular response, Journal of Endodontics 34 (2008) 39–44.
[19] J.E. Gomes-Filho, G. Rodrigues, S. Watanabe, P.F.E. Bernabé, C.S. Lodi, A.C. Gomes, M.D. Faria, A.D. Dos Santos, J.C.S. Moraes, Evaluation of the tissue reaction to fast endodontic cement (CER) and Angelus MTA, Journal of Endodontics 10 (2009) 351377–351380.
[20] A.D. Santos, E.B. Araújo, K. Yukimitu, J.C. Barbosa, J.C.S. Moraes, Setting time and thermal expansion of two endodontic cements, Oral Surgery, Oral Medicine, Oral Pathology, Oral Radiology and Endodontology 106 (2008) 77–79.
[21] J.S. Song, F.K. Mante, W.J. Romanow, S. Kim, Chemical analysis of powder and set forms of Portland cement, Gray ProRoot MTA, White ProRoot MTA and Gray MTA-Angelus, Oral Surgery, Oral Medicine, Oral Pathology, Oral Radiology and Endodontology 102 (2006) 809–815.
[22] B.J. Christensen, R.T. Coverdale, R.A. Olson, S.J. Ford, E.J. Garboczi, H.M. Jennings, T.O. Mason, Impedance spectroscopy of hydrating cement-based materials: measurement, interpretation and application, Journal of the American Ceramic Society 77 (1994) 2789–2804.
[23] P. Gu, P. Xie, J.J. Beaudoin, R. Brousseau, A.C. impedance spectroscopy (I): a new equivalent circuit model for hydrated Portland cement paste, Cement and Concrete Research 22 (1992) 833–840.
[24] P. Xie, P. Gu, Z. Xu, J.J. Beaudoin, A rationalized A.C. impedance model for microstructural characterization of hydrating cement systems, Cement and Concrete Research 23 (1993) 359–367.
[25] J.H. Hwang, Impedance spectroscopy analysis of hydration in ordinary Portland cements involving chemical mechanical planarization slurry, Journal of the Korean Ceramic Society 49 (2012) 260–265.
[26] Y. Arai, Semento No Zairyo Kagaku, 2nd ed., Dainippon Tosho Publishing Co. Ltd, Chuo-ku, Tokyo, Japan, 1990 (in Japanese).
[27] C. Villat, V.X. Tran, N. Pradelle-Plasse, P. Ponthiaux, F. Wenger, B. Grosgogeat, P. Colon, Impedance methodology: a new way to characterize the setting of dental cements, Dental Materials 26 (2010) 1127–1132.
[28] S.J. Ford, J.H. Hwang, J.D. Shane, R.A. Olson, G.M. Moss, H.M. Jennings, T.O. Mason, Dielectric amplification in cement pastes, Advanced Cement Based Materials 5 (1997) 41–48.